Quantifying uncertainty in state and parameter estimation

Ulrich Parlitz, Jan Schumann-Bischoff, and Stefan Luther

Max Planck Institute for Dynamics and Self-Organization Am Faßberg 17, 37077 Göttingen, Germany and Institute for Nonlinear Dynamics, Georg-August-Universität Göttingen, Am Faßberg 17, 37077 Göttingen, Germany (Received 20 November 2013; published 15 May 2014)

Observability of state variables and parameters of a dynamical system from an observed time series is analyzed and quantified by means of the Jacobian matrix of the delay coordinates map. For each state variable and each parameter to be estimated, a measure of uncertainty is introduced depending on the current state and parameter values, which allows us to identify regions in state and parameter space where the specific unknown quantity can(not) be estimated from a given time series. The method is demonstrated using the Ikeda map and the Hindmarsh-Rose model.

DOI: 10.1103/PhysRevE.89.050902 PACS number(s): 05.45.Tp, 05.45.Xt

In physics and other fields of science including quantitative biology, life sciences, and climatology, mathematical models play a crucial role for understanding and predicting dynamical processes. In the following we assume that such a model exists and is known. But even in the ideal case of a model obtained from fundamental physical laws this model typically contains some parameters whose values have to be determined depending on the physical context. Furthermore, not all state variables of the model may be easily experimentally accessible. To estimate the unknown parameters and state variables you may either devise specific experiments focusing on the quantity of interest or you can try to extract the required information from a measured time series of the process to be modeled. Technically, several estimation methods exist, including observer or synchronization schemes [1–6], particle filters [7], a path integral formalism [8,9], or optimization based algorithms [10–12]. However, these methods may fail and at this point the question arises whether the failure is due to the specific algorithm used or due to a lack of information in the available time series. In this article we address the second option and present a general approach for answering the question whether a given time series enables the estimation of parameters or variables of interest in a given model. The mathematical tool that is used to answer this question is delay reconstruction [13-17] and the basic criterion for local observability is the rank of the Jacobian matrix of the delay coordinates map. This approach was motivated by work of Letellier, Aguirre, and Maquet [18–20] who studied the question which state variables can be estimated or observed from a given time series using derivative coordinates. Observability of (continuous) dynamical systems is also a major issue in control theory [21-23] and nonlinear time series analysis [24]. Here we consider discrete time and delay coordinates, and we introduce a quantitative measure of uncertainty, which in general varies on the attractor and thus indicates where in state space estimation is more efficient and less error prone. Furthermore, we focus not only on state variables but also on observability of model parameters.

Let's assume, first, that our model of interest is a *M*-dimensional discrete dynamical system,

$$\mathbf{x}(n+1) = \mathbf{g}[\mathbf{x}(n), \mathbf{p}],\tag{1}$$

given by an iterated function **g** depending on the state vector $\mathbf{x}(n) = [x_1(n), \dots, x_M(n)] \in \mathbb{R}^M$ at time n and K parameters $\mathbf{p} = (p_1, \dots, p_K) \in \mathbb{R}^K$. This system generates the times series $\{s(n)\}$ with $s(n) = h[\mathbf{x}(n)]$ (for $n = 1, \dots, N$), where h denotes a measurement or observation function. The time series $\{s(n)\}$ can be used to construct a D-dimensional delay reconstruction [13–17],

$$\mathbf{y}(n) = [s(n), s(n+1), \dots, s(n+D-1)]$$
$$= G(\mathbf{x}(n), \mathbf{p}) \in \mathbb{R}^{D}, \tag{2}$$

providing the *delay coordinates map* $G : \mathbb{R}^{M+K} \to \mathbb{R}^{D}$.

To uniquely recover the full state \mathbf{x} and the parameters \mathbf{p} from the observations represented by the reconstructed state \mathbf{y} , we require the map G to be smooth and locally invertible. More precisely, let $M+K \leq D$ and let $(\mathbf{x},\mathbf{p}) \in \mathcal{U}$ where $\mathcal{U} \subset \mathbb{R}^{M+K}$ is a smooth manifold. Then G is locally invertible on the image $G(\mathcal{U}) \subset \mathbb{R}^D$ if the $D \times (M+K)$ Jacobian matrix $DG(\mathbf{x},\mathbf{p})$ has full rank M+K (i.e., G is an immersion [15]).

The map from delay reconstruction space \mathbb{R}^D to the state and parameter space \mathbb{R}^{M+K} is locally given by the (pseudo) inverse of the Jacobian matrix DG of the delay coordinates map G, which can be computed using a singular value decomposition

$$DG = USV^{\text{tr}} \tag{3}$$

where $S = \operatorname{diag}(\sigma_1, \ldots, \sigma_{M+K})$ is a $(M+K) \times (M+K)$ diagonal matrix containing the singular values $\sigma_1 \geqslant \sigma_2 \geqslant \cdots \geqslant \sigma_{M+K} \geqslant 0$ and $U = [\mathbf{u}^{(1)}, \ldots, \mathbf{u}^{(M+K)}]$ and $V = [\mathbf{v}^{(1)}, \ldots, \mathbf{v}^{(M+K)}]$ are orthogonal matrices, represented by the column vectors $\mathbf{u}^{(i)} \in \mathbb{R}^D$ and $\mathbf{v}^{(i)} \in \mathbb{R}^{M+K}$, respectively. V^{tr} is the transposed of V coinciding with the inverse $V^{-1} = V^{\text{tr}}$. Analogously, $U^{\text{tr}} = U^{-1}$ and the (pseudo) inverse Jacobian matrix reads $DG^{-1} = VS^{-1}U^{\text{tr}}$ where $S^{-1} = \operatorname{diag}(1/\sigma_1, \ldots, 1/\sigma_{M+K})$. Multiplying by U from the right we obtain $DG^{-1}U = VS^{-1}$ or

$$DG^{-1}\mathbf{u}^{(j)} = \frac{1}{\sigma_j}\mathbf{v}^{(j)} \quad (j = 1, \dots, M + K).$$
 (4)

In Fig. 1 the transformation of singular vectors Eq. (4) is illustrated for the case M = 2 and K = 0 (no unknown parameters). The diagram shows how small perturbations of \mathbf{y} in delay reconstruction space result in deviations from \mathbf{x} in the original state space. Most relevant for the local observability of

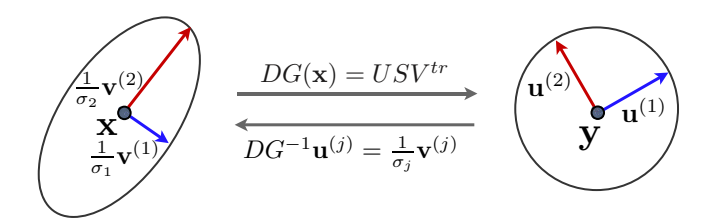


FIG. 1. (Color online) The (pseudo) inverse Jacobian matrix $DG^{-1}(\mathbf{y})$ maps perturbations of \mathbf{y} in delay reconstruction space to deviations from the state \mathbf{x} whose magnitudes depend on the direction of the perturbation as described by Eq. (4).

the (original) state \mathbf{x} is the length of the longest principal axis of the ellipsoid given by the inverse of the smallest singular value σ_2 (see Fig. 1). Small singular values correspond to directions in state space, where it is difficult (or even impossible) to locate the true state \mathbf{x} given a finite precision of the reconstructed state \mathbf{y} . The ratio $\sigma_{\min}/\sigma_{\max}$ of the smallest and the largest singular value is a measure of observability at the reference state \mathbf{x} . By averaging on the attractor we define (analogously to a similar definition for derivative coordinates [18,19]) the *observability index*

$$\bar{\gamma} = \frac{1}{N} \sum_{n=1}^{N} \frac{\sigma_{\min}^2(\mathbf{x}(n))}{\sigma_{\max}^2(\mathbf{x}(n))}.$$
 (5)

If the perturbations of **y** are due to normally distributed measurement noise then they can be described by a symmetric Gaussian distribution centered at **y**,

$$Q(\tilde{\mathbf{y}}) = \frac{\exp\left[-\frac{1}{2}(\tilde{\mathbf{y}} - \mathbf{y})^{\text{tr}} \Sigma_{y}^{-1}(\tilde{\mathbf{y}} - \mathbf{y})\right]}{\sqrt{(2\pi)^{D} \det(\Sigma_{y})}},$$
 (6)

where $\tilde{\mathbf{y}}$ is the perturbed state, $\Sigma_y = \operatorname{diag}(\rho^2, \ldots, \rho^2) = \rho^2 I_D$ denotes the $D \times D$ covariance matrix $(I_D \text{ stands for the } D \text{-dimensional unit matrix})$, and the standard deviation ρ quantifies the noise amplitude. For (infinitesimally) small perturbations $\Delta \mathbf{y} = \tilde{\mathbf{y}} - \mathbf{y}$, this distribution is mapped by the pseudo inverse of the linearized delay coordinates map to the (nonsymmetrical) distribution

$$P(\tilde{\mathbf{x}}) = \frac{\exp\left[-\frac{1}{2}(\tilde{\mathbf{x}} - \mathbf{x})^{\text{tr}} \Sigma_{x}^{-1} (\tilde{\mathbf{x}} - \mathbf{x})\right]}{\sqrt{(2\pi)^{M+K} \det(\Sigma_{x})}},$$
 (7)

centered at x with the inverse covariance matrix

$$\Sigma_x^{-1} = DG^{\text{tr}} \Sigma_y^{-1} DG$$

$$= \frac{1}{\rho^2} DG^{\text{tr}} DG = \frac{1}{\rho^2} VS^2 V^{\text{tr}}.$$
(8)

The marginal distribution P_j of the jth state variable centered a x_j is given by

$$P_j(\tilde{x}_j) = \frac{1}{\rho_i \sqrt{2\pi}} \exp\left[-\frac{(\tilde{x}_j - x_j)^2}{2\rho_i^2}\right],\tag{9}$$

where the standard deviation ρ_j is given by the square root of the diagonal elements of the covariance matrix $\rho_j = \sqrt{\Sigma_{x,jj}}$ that can be obtained by inverting Σ_x^{-1} [given in Eq. (8)]. Since the noise level ρ of the observations appears in Eq. (8) as a

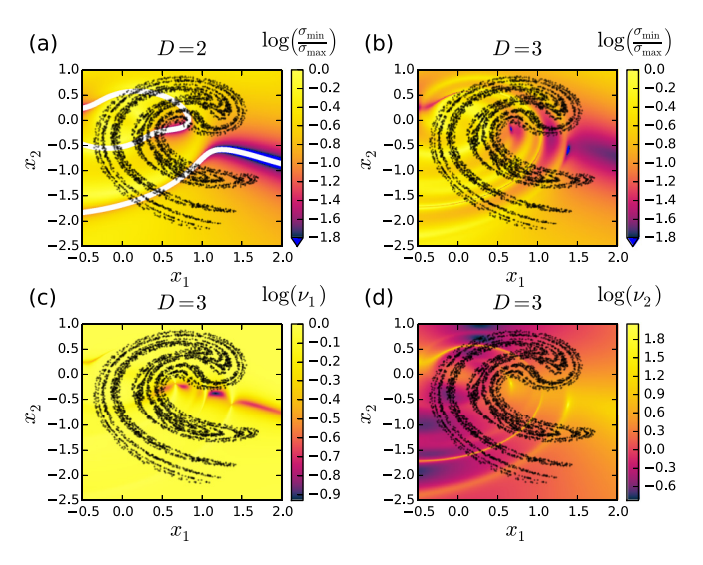


FIG. 2. (Color online) Observability of the state variables x_1 and x_2 of the Ikeda map Eq. (11) from a x_1 time series (with known parameters, K=0, M=2). (a), (b) Color-coded ratio of singular values $\sigma_{\min}/\sigma_{\max}$ vs. x_1 and x_2 for reconstruction dimension D=2 (a) and D=3 (b). The white curves in (a) indicate the location of zeros of $\det(DG)$. (c), (d) Color-coded uncertainties v_1 (c) and v_2 (d) of x_1 and x_2 estimates, respectively. Note the logarithmic color axes. Black dots represent the Ikeda attractor.

factor only we can, without loss of generality, choose $\rho=1$ and use

$$v_j = \sqrt{[DG^{\text{tr}}DG]_{jj}^{-1}} = \sqrt{[VS^{-2}V^{\text{tr}}]_{jj}}$$
 (10)

as a measure of *uncertainty* when estimating x_j , which can be interpreted as a noise amplification factor. The same reasoning holds for the unknown parameters **p**.

To illustrate this quantification of observability, we first consider the Ikeda map [25] $z(n+1) = p_1 + p_2 z(n) \exp[ip_3 - ip_4/(1+|z(n)|^2)]$ with $z(n) = x_1(n) + ix_2(n) \in \mathbb{C}$ that can also be written as

$$x_1(n+1) = p_1 + p_2[x_1(n)\cos\theta_n - x_2(n)\sin\theta_n]$$

$$x_2(n+1) = p_2[x_1(n)\sin\theta_n + x_2(n)\cos\theta_n],$$
 (11)

where $\theta_n = p_3 - p_4/[1 + x_1^2(n) + x_2^2(n)]$. For the standard parameters $p_1 = 1$, $p_2 = 0.9$, $p_3 = 0.4$, and $p_4 = 6$, this map generates the chaotic attractor shown in Fig. 2.

First, we consider a case where all parameters are known and only the variables x_1 and x_2 have to be estimated from the observable $s(n) = x_1(n)$ (i.e., M = 2 and K = 0). Figures 2(a) and 2(b) show (color-coded) the ratio of the smallest singular value $\sigma_{\min} = \sigma_M$ and the largest singular value $\sigma_{\max} = \sigma_1$ of the Jacobian matrix $DG(\mathbf{x})$ of the delay coordinates map versus x_1 and x_2 . Reconstruction dimensions are D = 2 in Fig. 2(a) and D = 3 in Fig. 2(b), respectively. For D = 2, the white curves indicate the zeros of the determinant of $DG(\mathbf{x}, \mathbf{p})$ that are computed as contour lines. As can be seen, parts of the Ikeda attractor cross these singularity manifolds or are close to regions in state space where the ratio $\sigma_{\min}/\sigma_{\max}$ is very close to zero, indicating an almost singular Jacobian matrix DG. There, state estimation is not possible, a fact that reconfirms previous results indicating that reconstruction dimensions D > 2 are

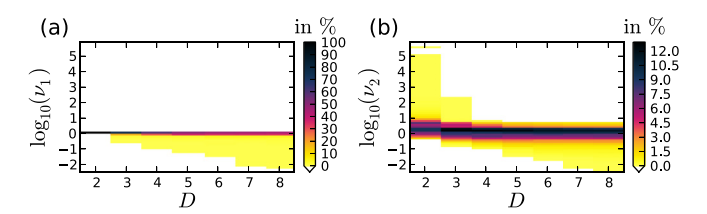


FIG. 3. (Color online) Histograms (color-coded) of uncertainties v_1 (a) and v_2 (b) computed from a x_1 time series of length $N=1000\,000$ generated on the attractor of the Ikeda map Eq. (11) with reconstruction dimensions ranging from D=2 to D=7. The state variables x_1 and x_2 are estimated (M=2), while all parameters are assumed to be known (K=0).

required for the Ikeda map [26]. For D=3, the singularities disappear and only some regions with relatively low ratios $\sigma_{\min}/\sigma_{\max}$ remain.

Figures 2(c) and 2(d) show v_1 and v_2 versus x_1 and x_2 , respectively. For both variables their uncertainties v_k vary and there are regions of low v_1 but relatively large v_2 .

Figures 3(a) and 3(b) show histograms of v_1 and v_2 for different reconstruction dimensions D, which were obtained from an orbit of length $N=1\,000\,000$ on the Ikeda attractor. Due to the choice $s(n)=x_1(n)$ the uncertainty v_1 of x_1 is for all dimensions equal or less than one. For D=2 the uncertainty v_2 of v_2 reaches very high values $v_2>10^6$ when the orbit passes those regions in state space where the Jacobian matrix $v_2>10^6$ is (almost) singular [see Fig. 2(a)]. For reconstruction dimensions $v_2>10^6$ indicating a significant improvement and for $v_2>10^6$ indicating a significant improvement and for $v_2>10^6$ indicating a significant improvement and for $v_2>10^6$ indicating a value that doesn't change anymore if the reconstruction dimension is increased furthermore. This feature is in very good agreement with previous results obtained when estimating Lyapunov exponents from Ikeda time series [26].

To obtain the histograms shown in Fig. 3 and in the following figures the model equations are used to generate a trajectory which provides a representative sample and subset of the attractor (similar to numerical computations of Lyapunov exponents).

For the results shown in Figs. 3(a) and 3(b) only the state variables are estimated and all parameters are assumed to be known (M = 2, K = 0). Figure 4 shows also the uncertainties ν_3 , ν_4 , ν_5 , and ν_6 of the parameters p_1 , p_2 , p_3 , and p_4 for an estimation task where all variables (M = 2) and all parameters (K = 4) are unknown. For increasing reconstruction dimension D, the distributions of all uncertainties converge with monotonically decreasing upper bounds (largest ν values quantifying large uncertainty of estimates at specific locations on the attractor).

Delay reconstruction can also be applied to observables $s(t) = h[\mathbf{x}(t)]$ from continuous dynamical systems,

$$\dot{\mathbf{x}} = \mathbf{f}(\mathbf{x}, \mathbf{p}),\tag{12}$$

using a suitable *delay time* τ :

$$\mathbf{y} = \{s(t), s(t+\tau), \dots, s[t+(D-1)\tau]\} = G(\mathbf{x}, \mathbf{p}) \in \mathbb{R}^{D}.$$

The Jacobian matrix $DG(\mathbf{x}, \mathbf{p})$ of the delay coordinates map G can be computed by solving linearized equations providing

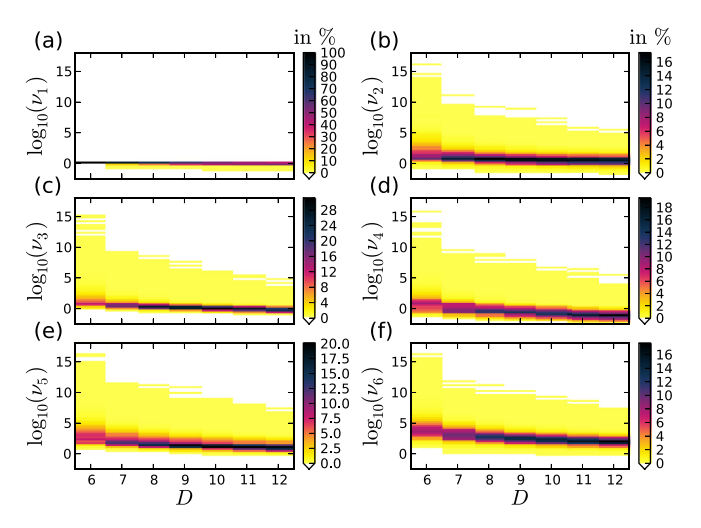


FIG. 4. (Color online) Histograms (color-coded) of uncertainties of state and parameter estimates of the Ikeda map Eq. (11) for reconstruction dimensions ranging from D=6 to D=12. Distributions are computed from a x_1 time series of length $N=1\,000\,000$ generated on the Ikeda attractor. All variables (M=2) and all parameters (K=4) are assumed to be unknown.

the Jacobian matrices $D_x \phi^t(\mathbf{x}, \mathbf{p})$ and $D_p \phi^t(\mathbf{x}, \mathbf{p})$ of the flow ϕ^t generated by the system Eq. (12) [27]. To demonstrate the application of the proposed uncertainty analysis to continuous time system we use the Hindmarsh-Rose (HR) neuron model [28]

$$\dot{x}_1 = -x_1^3 + p_1 x_1^2 + x_2 - x_3
\dot{x}_2 = 1 - p_2 x_1^2 - x_2
\dot{x}_3 = p_3 [x_1 + p_4 (p_5 - x_3)].$$
(13)

For parameter values $p_1 = 3$, $p_2 = 5$, $p_3 = 0.004$, $p_4 = 3.19$, $p_5 = 0.25$ the HR model exhibits chaotic bursting of x_1 and x_2 and slow variations of x_3 [11].

Figures 5(a) and 5(b) show the dependence of probability distributions (color-coded) of uncertainties v_2 , and v_3 , respectively, on the delay time τ chosen for performing the delay reconstruction. The reconstruction dimension equals D=7. With this example, all parameters are assumed to be known (K = 0) and the first state variable is chosen as measured time series $s(t_n) = x_1(t_n)$ with $t_n = n\tau$. Therefore, the estimation of x_1 is not much affected by the choice of the delay time and $v_1 \le 1$ (with $v_1 \approx 1$ most of the time, not shown here). As can be seen, the centers of both distributions decrease monotonically with τ indicating an improvement of the estimation accuracy for larger delay times. Figures 5(c) and 5(d) show histograms (color-coded) of uncertainties v_2 and v_3 versus reconstruction dimension D for $\tau = 0.1$. Larger D provides lower uncertainties v_i and compared to Figs. 5(a) and 5(b) very large v_i do not occur anymore. Note that corresponding columns of Figs. 5(a) and 5(b) and Figs. 5(c) and 5(d), respectively, are computed using delay coordinates covering the same window in time ranging from $\tau(D-1) = 0.1 \times 6 = 0.6$ to $\tau(D-1) = 30.1 \times 6 =$ $1806 \times 0.1 = 180.6$. The more densely sampling $(\tau = 0.1)$ underlying Figs. 5(c) and 5(d) provides more information about the underlying dynamics and results in lower uncertainty

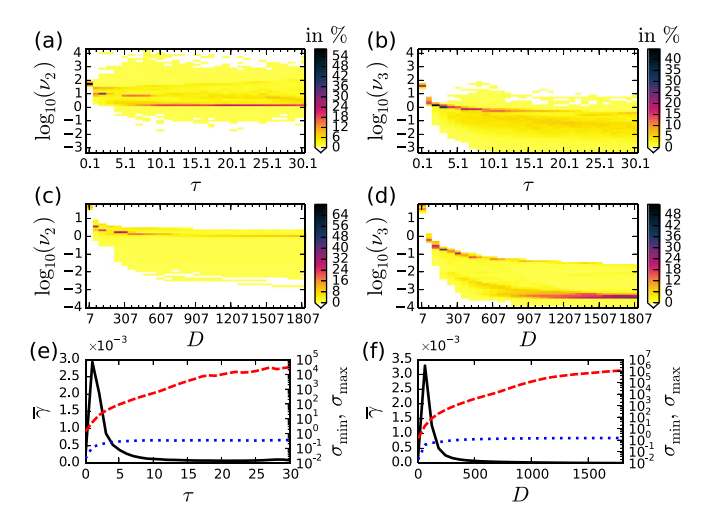


FIG. 5. (Color online) Probability distributions (color-coded) of uncertainties v_2 and v_3 when estimating the state variables x_1 , x_2 , and x_3 of the HR model Eq. (13) from a x_1 time series. In (a) and (b) the delay reconstruction dimension is fixed at D=7 and the delay τ is varied. (c), (d) Distributions for $\tau=0.1$ and different reconstruction dimensions D. Corresponding columns (histograms) of all four diagrams show results for the same window in time (D-1) τ used upon delay reconstruction. (e), (f) Observability index $\tilde{\gamma}$ (5) (solid curve), σ_{\min} (dotted curve), and σ_{\max} (dashed curve) vs. τ and vs. D.

values. Figures 5(e) and 5(f) show the observability index $\bar{\gamma}$ Eq. (5) and mean values of the smallest and the largest singular values σ_{\min} and σ_{\max} versus τ and D, respectively. While $\bar{\gamma}$ exhibits a clear peak, σ_{\min} converges to an asymptotic value, and σ_{\max} increases monotonically, i.e., the lengths of the ellipsoid axes in Fig. 1 decrease $(1/\sigma_{\max})$ or converge $(1/\sigma_{\min})$.

If in addition to the three state variables x_1 , x_2 , and x_3 also the five parameters p_1, \ldots, p_5 of the HR-model Eq. (13) are to be estimated from the x_1 time series then we have to cope with an estimation task with M + K = 3 + 5 = 8uncertainties whose distributions for $\tau = 0.1$ are shown in Fig. 6 for delay reconstruction dimensions ranging from D=8to D = 2008. For increasing D the uncertainties v_1, \ldots, v_6 corresponding to $x_1, x_2, x_3, p_1, p_2, p_3$ decrease to values close to or below one. The uncertainties v_7 and v_8 of parameters p_4 and p_5 , respectively, remain rather large (>1000) even for high-dimensional reconstructions. This feature indicates that it is very difficult to estimate both parameters together. In fact, if p_4 (or p_5) is known and only p_5 (or p_4) has to be estimated (together with $x_1, x_2, x_3, p_1, p_2, p_3$) then the uncertainty values of p_5 (or p_4) are much smaller and lie in the range of the uncertainties of the other parameters. Applying a state and parameter estimation algorithm [11,29] we also encountered problems (in terms of large deviations from the true values) when trying to estimate both parameters p_4 and p_5 together. These two parameters are to some degree redundant in the sense that different combinations yield (almost) the same

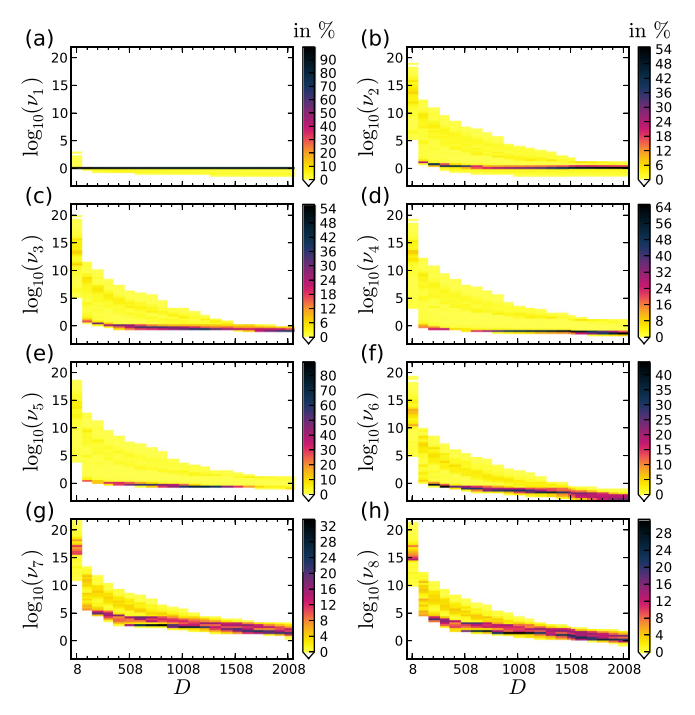


FIG. 6. (Color online) Distributions of uncertainties v_j vs. reconstruction dimension D obtained for the HR model Eq. (13) where all three state variables and all five parameters are estimated from a x_1 time series. The delay time $\tau = 0.1$ is fixed.

 x_1 time series and thus cannot be clearly distinguished using a x_1 time series, only.

The presented approach for quantifying uncertainties of model-based state and parameter estimation from time series provides a general criterion whether and how reliably specific model variables and parameters can be estimated from time series. This method is independent from any particular estimation method and it can be extended in several ways, including unknown parameters in the measurement function and multivariate time series. High uncertainty implies that the corresponding quantity of the model has small impact on the output and may thus be a candidate for reducing the formal model complexity by pruning. Furthermore, the information provided by the values of uncertainty can be exploited to improve state and parameter estimation methods.

ACKNOWLEDGMENTS

The research leading to these results has received funding from the European Community's Seventh Framework Program FP7/2007-2013 under grant agreement no. HEALTH-F2-2009-241526, EUTrigTreat. We acknowledge financial support by the German Federal Ministry of Education and Research (BMBF) Grant No. 031A147, the Deutsche Forschungsgemeinschaft (SFB 1002: Modulatory Units in Heart Failure), and by the German Center for Cardiovascular Research (DZHK e.V.).

^[1] H. Nijmeijer and I. M. Y. Mareels, IEEE Trans. Circuits Syst. I 44, 882 (1997).

^[2] H. J. C. Huijberts, T. Lilge, and H. Nijmeijer, Int. J. Bif. Chaos 11, 1997 (2001).

- [3] U. Parlitz, L. Junge, and L. Kocarev, Phys. Rev. E 54, 6253 (1996).
- [4] D. Ghosh and S. Banerjee, Phys. Rev. E 78, 056211 (2008).
- [5] H. D. I. Abarbanel, D. R. Creveling, and J. M. Jeanne, Phys. Rev. E 77, 016208 (2008).
- [6] F. Sorrentino and E. Ott, Chaos 19, 033108 (2009).
- [7] P. J. van Leeuwen, Q. J. R. Meteorol. Soc. 136, 1991 (2010).
- [8] H. D. I. Abarbanel, Phys. Lett. A 373, 4044 (2009).
- [9] J. C. Quinn and H. D. I. Abarbanel, Q. J. R. Meteorol. Soc. 136, 1855 (2010).
- [10] D. R. Creveling, P. E. Gill, and H. D. I. Abarbanel, Phys. Lett. A 372, 2640 (2008).
- [11] J. Schumann-Bischoff and U. Parlitz, Phys. Rev. E 84, 056214 (2011).
- [12] J. Bröcker, Q. J. R. Meteorol. Soc. 136, 1906 (2010).
- [13] D. Aeyels, SIAM J. Contr. Optimiz. 19, 595 (1981).
- [14] F. Takens, Lect. Notes Math. 898, 366 (1981).
- [15] T. Sauer, J. A. Yorke, and M. Casdagli, J. Stat. Phys. 65, 579 (1991).
- [16] H. Kantz and T. Schreiber, *Nonlinear Time Series Analysis*, Cambridge Nonlinear Science Series 7 (Cambridge University Press, Cambridge, 1997).

- [17] H. D. I. Abarbanel, Analysis of Observed Chaotic Data (Springer Verlag, Berlin, 1997), 2nd ed.
- [18] C. Letellier, L. A. Aguirre, and J. Maquet, Phys. Rev. E 71, 066213 (2005); Comm. Nonl. Sci. Num. Sim. 11, 555 (2006).
- [19] C. Letellier and L. A. Aguirre, Phys. Rev. E 79, 066210 (2009).
- [20] M. Frunzete, J.-P. Barbot, and C. Letellier, Phys. Rev. E 86, 026205 (2012).
- [21] R. Hermann and A. J. Krener, IEEE Trans. Autom. Contr. AC-22, 728 (1977).
- [22] E. D. Sontag, Mathematical Control Theory: Deterministic Finite Dimensional Systems (Springer, New York, 1998), 2nd ed
- [23] H. Nijmeijer, Int. J. Control 36, 867 (1982).
- [24] H. U. Voss, J. Timmer, and J. Kurths, Int. J. Bif. Chaos 14, 1905 (2004).
- [25] K. Ikeda, Opt. Commun. 30, 257 (1979).
- [26] P. Bryant, R. Brown, and H. D. I. Abarbanel, Phys. Rev. Lett. 65, 1523 (1990).
- [27] H. Kawakami, IEEE Trans. Circ. Syst. CAS-31, 248 (1984).
- [28] J. L. Hindmarsh and R. M. Rose, Proc. R. Soc. Lond. B 221, 87 (1984).
- [29] J. Schumann-Bischoff, S. Luther, and U. Parlitz, Commun. Nonlin. Sci. Num. Sim. 18, 2733 (2013).